Local-field effect in the second-harmonic-generation spectra of Si surfaces

Bernardo S. Mendoza
Centro de Investigaciones en Optica, A.C. Apartado Postal 1-948, 37000 León, Guanajuato, Mexico

W. Luis Mochán
Laboratorio de Cuernavaca, Instituto de Física, Universidad Nacional Autónoma de México, Apartado Postal 48-3, 62251 Cuernavaca, Morelos, Mexico

(Received 15 December 1995; revised manuscript received 16 February 1996)

We calculate the second-harmonic-generation spectra of Si(100) and (111) surfaces introducing the nonlinear surface local-field effect. Our model consists of four interpenetrated fcc lattices of polarizable bonds, each of which is centrosymmetric, but responds nonlinearly to the spatial inhomogeneities of the polarizing local field. The gradient of the field induced at a bond due to the dipole moment of a neighbor leads to a second-order polarization that is canceled out in the bulk after summing over all other bonds, but it is not compensated at the surface, where it leads to a large nonlinear macroscopic response. Our model parameters are fitted to the nonlinear anisotropy measured at 1.17 and 2.34 eV. The linear anisotropy spectra calculated for the Si(110) surface are in accordance with reflectance difference measurements. The same parameters yield a nonlinear spectrum that has peaks at 1.65 eV for a strained (100) surface and at 1.75 eV for a (111) surface, in agreement with recent experimental results. [S0163-1829(96)53516-2]

Surface optical second-harmonic generation (SHG) is a useful nondestructive surface probe, since the electric-dipolar quadratic response within the bulk of centrosymmetric systems is symmetry forbidden. Therefore a large portion of the light with frequency 2ω reflected from an interface illuminated with monochromatic radiation at ω is surface originated. An added advantage is the possibility of accessing surfaces such as buried interfaces, out of ultrahigh vacuum conditions and within arbitrary transparent ambients. However, the efficiency of the surface SHG is extremely low, typically of the order of 10^{-20} cm^2/W, and therefore very powerful laser systems are required for its observation. For this reason, most experiments have been performed at a few selected frequencies such as the intense 1.17-eV line of the Nd-YAG (yttrium aluminum garnet) laser and its second harmonic, emphasizing the polar and azimuthal angular dependence of the signal for different crystal surfaces and combinations of incoming and outgoing polarizations[1–11] over its frequency dependence. The possible angular dependence of SHG is well understood in terms of the independent components of the bulk and surface nonlinear susceptibilities and their symmetry originated constraints.[12–14]

Recently, the development of high power tunable lasers with a wide spectral range has stimulated experiments in nonlinear surface spectroscopy. In particular, SHG spectra have been measured for different clean, oxidized and adsorbate-covered surfaces of Si.[15,16] These spectra show a well developed peak close to $2\hbar\omega = 3.3$ eV, whose position and relative insensitivity to surface conditions suggests that it is originated from a bulk transition between the valence and conduction bands which becomes SH electric-dipolarly active due to distortions in the crystalline structure close the surface.[15]

The purpose of the present paper is the development of a simple quantitative theory for the SHG spectra of semiconductor surfaces accounting in an approximate way for the bulk transitions and the crystalline symmetry. A previous successful theory for the surface linear response of natural Si incorporated the geometrical arrangement of the atoms at the surface through the surface local-field effect.[17] In this paper we extend that theory to the nonlinear response. We expect the local-field effect to have large consequences in SHG through the following mechanism: Consider a localized polarizable entity and a semi-infinite crystal made up of its replicas. If each entity is centrosymmetric it would have no electric-dipole-allowed SH transition, though it may have electric-quadrupolar and magnetic-dipolar contributions proportional to $\vec{\mathscr{E}}_i \nabla \vec{\mathscr{E}}_i$, where $\vec{\mathscr{E}}_i$ is the local field acting at site i. The external field has a very slow spatial variation whose scale is of the order of the wavelength λ, although the field induced by a nearby entity j may have a very large variation, with a scale determined by the distance from j to i, r_{ij} which of course is of atomic dimensions a. Different neighbors contribute to the gradient $\nabla \vec{\mathscr{E}}_i$ along different directions, so that, if the site i is itself centrosymmetric, these large gradients will cancel out among themselves, leaving only a small residual gradient of order $\mathscr{E}/\lambda$. This cancellation is no longer possible at the surface, where $|\nabla \vec{\mathscr{E}}| \approx \mathscr{E}/a$, yielding a large SH surface polarization. When written in terms of the macroscopic field $\vec{E}$ this surface polarization is then proportional to $\vec{E}\vec{E}/a$ which corresponds to a large surface-allowed dipolar SH processes. In this paper we develop the model above into a full calculation for Si surfaces, building upon a previous paper by Schaich and Mendoza.[18]

The semiconductor that we study has a simple diamond-like structure, with a tetrahedron as the basic unit. This unit can be viewed as a cube with one atom at the center linked through four bonds to atoms sitting at alternate corners. The diamond structure is constructed by replicating these four bonds into four intercalated fcc lattices. The polarization induced in the semiconductor originates from the displacement

of its charge distribution, which has strong maxima at the middle of each bond. Therefore, we model the crystal as a collection of lattices of anisotropic cylindrically symmetric centrosymmetric polarizable bonds. The nonlinear polarization $\vec{p}^{(\mathrm{tot})}_{n\lambda}(2\omega)$ of the nth site of the fcc lattice corresponding to the λth bond orientation ($\lambda=1,\ldots,4$) is given by

$$\vec{p}^{(\mathrm{tot})}_{n\lambda}(2\omega)=\vec{p}^{(\mathrm{nl})}_{n\lambda}(2\omega)+\overleftrightarrow{\alpha}^{\lambda}(2\omega)\cdot\left[\frac{1}{2}\sum_{n'\lambda'}\overleftrightarrow{N}_{n\lambda n'\lambda'}:\vec{Q}^{(\mathrm{nl})}_{n'\lambda'}(2\omega)+\sum_{n'\lambda'}\overleftrightarrow{M}_{n\lambda n'\lambda'}\cdot\vec{p}^{(\mathrm{tot})}_{n'\lambda'}(2\omega)\right], \tag{1}$$

where $[p^{(\mathrm{nl})}_{n\lambda}(2\omega)]_i=(\chi^{(p)\lambda}_{ijkl}+\chi^{(m)\lambda}_{ijkl})\mathscr{E}_j\nabla_k\mathscr{E}_l$ is the nonlinear polarization at 2ω due to the interaction of a single bond with nonlinear electric and magnetic dipolar susceptibility tensors $\vec{\chi}^{(p)}$ and $\vec{\chi}^{(m)}$ with the spatially varying linear local field $\vec{\mathscr{E}}$ evaluated at the center $\vec{r}_{n\lambda}$ of the bond, $\overleftrightarrow{\alpha}^{\lambda}$ is the linear anisotropic polarizability of the bond, with components $\alpha_{\parallel}$ and $\alpha_{\perp}$ along and perpendicular to the bond's axis, and the term within the square brackets is the local field at 2ω and it contains a quadrupole originated field and the field induced by the total nonlinear dipole moments of the other bonds. The quadrupole moment is $\vec{Q}^{(\mathrm{nl})}_{n\lambda}(2\omega)=\vec{\chi}^{(Q)\lambda}:\vec{\mathscr{E}}\vec{\mathscr{E}}$ where $\chi^{(Q)\lambda}$ is the quadrupolar susceptibility of the λth bond, and the dipole-dipole and quadrupole-dipole interaction tensors are

$$\overleftrightarrow{M}_{n\lambda n'\lambda'}=\nabla\nabla\frac{1}{|\vec{r}-\vec{r}_{n'\lambda'}|}\bigg|_{\vec{r}=\vec{r}_{n\lambda}}, \tag{2}$$

$$\overleftrightarrow{N}_{n\lambda n'\lambda'}=-\nabla\nabla\nabla\frac{1}{|\vec{r}-\vec{r}_{n'\lambda'}|}\bigg|_{\vec{r}=\vec{r}_{n\lambda}}. \tag{3}$$

The linear local field is

$$\vec{\mathscr{E}}_{n\lambda}=\left[\vec{E}^{(\mathrm{ext})}(\vec{r}_{n\lambda})+\sum_{n'\lambda'}\overleftrightarrow{M}_{n\lambda n'\lambda'}\cdot\vec{p}_{n'\lambda'}(\omega)\right], \tag{4}$$

where the linear polarization obeys $\vec{p}_{n\lambda}(\omega)=\overleftrightarrow{\alpha}^{\lambda}(\omega)\cdot\vec{\mathscr{E}}_{n\lambda}$.

For an anisotropic harmonic oscillator there are simple expressions relating the nonlinear susceptibilities $\vec{\chi}^{(p)}$, $\vec{\chi}^{(m)}$, and $\vec{\chi}^{(Q)}$ to the linear polarizability at the fundamental and at the second-harmonic frequencies $\overleftrightarrow{\alpha}(\omega)$ and $\overleftrightarrow{\alpha}(2\omega)$, namely, $\chi^{(p)}_{ijkl}(\omega)=[\alpha_{il}(2\omega)\alpha_{jk}(\omega)+\alpha_{ik}(2\omega)\alpha_{jl}(\omega)]/(2e)$, $\chi^{(m)}_{ijkl}(\omega)=3[\alpha_{il}(2\omega)\alpha_{jk}(\omega)-\alpha_{ik}(2\omega)\alpha_{jl}(\omega)]/(2e)$, and $\chi^{(Q)}_{ijkl}(\omega)=[\alpha_{il}(\omega)\alpha_{jk}(\omega)+\alpha_{ik}(\omega)\alpha_{jl}(\omega)]/(2e)$. We assume these relations to hold approximately for the bond susceptibilities of a Si crystal and further assume that $\overleftrightarrow{\alpha}^{\lambda}$ is independent of position. Therefore, in our model we incorporate only the surface modification to the local fields, and we ignore any other surface modification to the linear and nonlinear response such as those due to transitions involving surface states.

Due to the long wavelength of light, within the bulk the linear polarization $\vec{p}_{n\lambda}(\omega)$ is almost independent of n. This allows an analytical solution which relates the bulk dielectric function $\epsilon(\omega)$ to the principal polarizabilities $\alpha_{\parallel}$ and $\alpha_{\perp}$. This relation is a generalization of the Clausius-Mossotti (CM) relation to the diamond structure. Close to the visible spectrum, we expect that the main contributions to $\alpha_{\parallel}$ can be related to bonding-antibonding transitions, while $\alpha_{\perp}$ is due to transitions involving atomic states with different symmetry. We assume the latter have a larger resonant frequency than the former. Therefore we assume that $\alpha_{\perp}(\omega)$ may be described by a Lorentzian centered at some relatively high resonance frequency $\omega_{\perp}$ with a weight characterized by a frequency parameter ω_p. Having chosen these parameters, we solve the generalized CM relation for each frequency to obtain $\alpha_{\parallel}(\omega)$ in terms of the experimentally measured bulk dielectric function $\epsilon(\omega)$.[19] Having determined the polarizability, and therefore also the nonlinear susceptibilities, we solve the local-field equations to obtain first $\vec{p}_{n\lambda}(\omega)$, then $\vec{p}^{(\mathrm{nl})}_{n\lambda}(2\omega)$ and $\vec{Q}^{(\mathrm{nl})}_{n\lambda}(2\omega)$, which substituted into Eq. (1) yields the total nonlinear polarization $\vec{p}^{(\mathrm{tot})}_{n\lambda}(2\omega)$. The details of this procedure will be described elsewhere.[20] Finally, averaging $\vec{p}^{(\mathrm{tot})}_{n\lambda}(2\omega)$ we obtain the bulk and surface polarization $\vec{P}^{(B)}(2\omega)$ and $\vec{P}^{(s)}(2\omega)$ per unit volume and unit area, respectively, and from them the nonlinear surface and bulk susceptibilities and the SHG efficiency $R^{(2)}(\omega)$, defined as the quotient of the reflected intensity $I_r(2\omega)$ to the square $I_i(\omega)^2$ of the incident intensity.

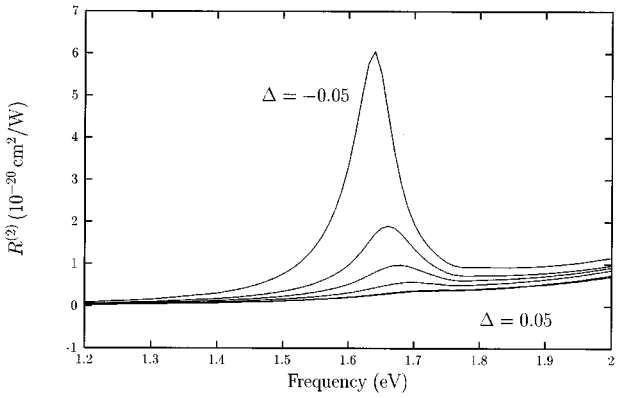

FIG. 1. SHG efficiency $R^{(2)}$ as function of frequency for Si(100). The angle of incidence is $\theta=45°$, the azimuthal angle is $\phi=30°$, and we chose $p\rightarrow P$ polarization. We present $R^{(2)}$ for $\Delta=+0.05,0,-0.025,-0.032,-0.042,-0.05$.

We chose the parameters $\hbar\omega_{\perp}=7.17$ eV and $\hbar\omega_p=1.68$ eV in order to reproduce the anisotropy of the SHG of Si(111) that has been measured for all possible combinations of incoming and outgoing s and p polarizations at $\hbar\omega=1.17$ eV and 2.34 eV.[1–4] Our value of $\omega_{\perp}$ is of the order of the transition energy between the atomic states of Si $3p^2\,{}^3P$ with $J=0$ and $3d^3D^0$ with $J=1$, in qualitative agreement with our argument above.[21] We have calculated[20] with these parameters the surface-induced anisotropy of the linear reflectance of Si(110) and found the result in agreement with experiment[22] and with a previous calculation which employed only one fcc lattice of tetrahedral isotropic polarizable entities.[17]

In Fig. 1 we show $R^{(2)}(\omega)$ calculated for light incident on Si(100) at an angle $\theta=45°$ with the plane of incidence at $\phi=30°$ from the [001] direction with $p(\mathrm{in})P(\mathrm{out})$ polarization. To account for strain within the first few layers, we have introduced a parameter $\Delta=d_1/d_B-1$, where d_B is the

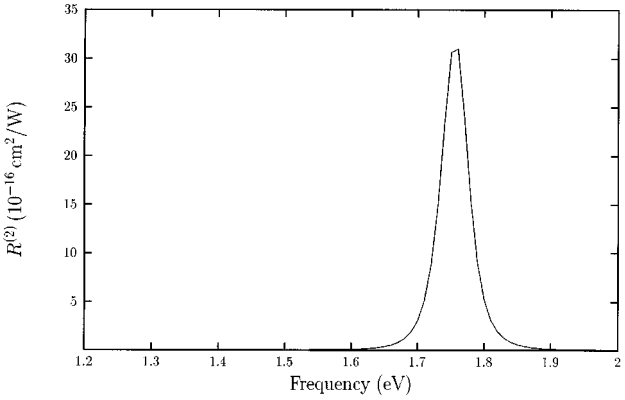

FIG. 2. SHG efficiency $R^{(2)}$ as a function of frequency for Si(111). The angle of incidence is $\theta=45°$, the azimuthal angle is $\phi=30°$, and we chose $p\rightarrow P$ polarization. In this case, $R^{(2)}$ is for the unstretched (111) surface.

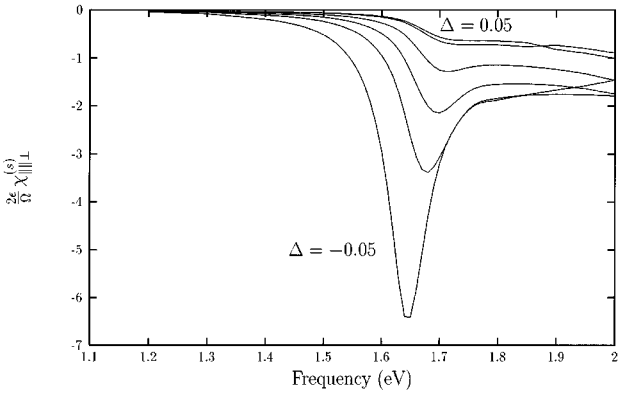

FIG. 3. Surface nonlinear susceptibility $\mathrm{Im}(\chi^{(s)}_{\parallel\parallel\perp})$ as a function of frequency for Si(100) corresponding to $\Delta=+0.05,0,\ -0.025,\ -0.032,\ -0.042,-0.05$.

separation between consecutive fcc planes in the bulk, and d_1 the corresponding separation between the first and second layers. For the bulk-truncated crystal ($\Delta=0$) we find a structureless spectrum, which is barely modified by stretching d_1. However, if we shrink d_1 by as little as 5% a very well developed peak appears at $\hbar\omega=1.65$ eV, with a width $\hbar\delta\omega\approx0.14$ eV, in excellent agreement with experiment. For even larger contractions the height of the peak increases but its position remains mostly unchanged. Therefore, it seems that the surface local field alone is able to explain the experimental findings on the flat, oxidized, strained Si(100) surfaces. Experiment shows a similar SHG spectrum for the clean (2×1) reconstructed surface.[15] A SHG spectrum calculation for a reconstructed surface would be desirable to understand the robustness of its structure. However, it would be impossible within our present formalism without introducing an unacceptable number of additional parameters to describe the polarizability of the topmost reconstructed layer.

In Fig. 2 we show $R^{(2)}(\omega)$ for Si(111) with $\theta=45°$ and $\phi=30°$ from the $[\bar{1}10]$ direction with $p(\mathrm{in})P(\mathrm{out})$ polarization. In this case even the undistorted crystal presents a peak at $\hbar\omega\approx1.75$ eV. Notice the huge change of scale between Figs. 1 and 2. The height of the latter peak is five orders of magnitude larger than that of the former.

An analysis of the different bulk and surface components of the nonlinear susceptibility reveals that the peak of Fig. 1 originates from a corresponding peak in $\chi^{(s)}_{\parallel\parallel\perp}=\partial^2P^{(s)}_{\parallel}(2\omega)/\partial E_{\parallel}\partial E_{\perp}$, which is displayed in Fig. 3 for different values of Δ. A similar analysis shows that the peak in Fig. 2 has contributions from $\chi^{(s)}_{\parallel\parallel\perp}$, $\chi^{(s)}_{\perp\parallel\parallel}$, and $\chi^{(s)}_{\parallel\parallel\parallel}$.

Finally, in Fig. 4 we show the polarization profile $[\vec{p}^{(\mathrm{tot})}_{n\lambda}(2\omega)]_{\parallel}$ corresponding to the efficiency maximum of the (100) face, i.e., the peak of Fig. 1. Notice that the total nonlinear polarization is largest in the second crystalline plane, after which it decays towards the negligible bulk polarization. This could explain the lack of sensitivity of this resonant peak to the surface condition. We have recalculated the SHG spectra modifying arbitrarily the surface polarizabilities and have found that the presence of the peak is very robust,[20] though its position is slightly shifted and its height is diminished. A very large change, such as that expected for a fully hydrogenated surface, would be necessary to remove it.[15,23]

In summary, we developed a model for the surface SHG of crystals with the structure of diamond which takes into account the nonlinear polarization induced by the microscopic spatial variation of the linear local field. The inputs to our calculation are the bulk dielectric function, the geometry of the crystal, and two parameters describing the response of an individual bond in the direction normal to its axis. The latter were fitted to several SHG anisotropy measurements on the (100) and (111) surfaces and we verified that they yield a linear reflectance difference spectrum for the (110) surface in agreement with experiment. We remark that a similar model with only one fcc lattice of isotropic polarizable entities,[24,18] each representing a tetrahedral arrangement of bonds, cannot reproduce either the bulk SHG anisotropy which is evident in the experiments on the (100) surface[4] or the peak at 3.3 eV. Although we have neglected all effects due to the surface modification of the electronic structure, we have obtained agreement with the first experimental spectra

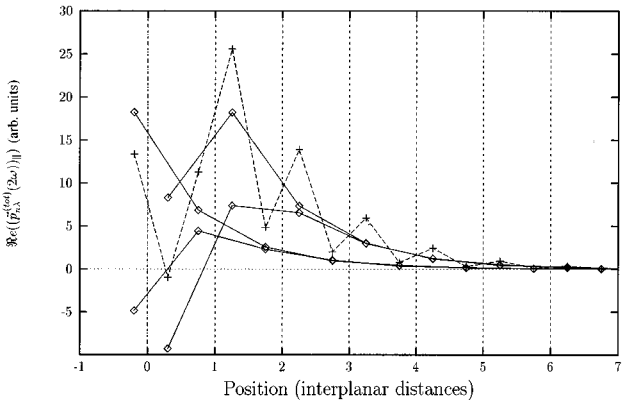

FIG. 4. Dipole moment $\mathrm{Re}[\{\vec{p}^{(\mathrm{tot})}_{n\lambda}(2\omega)\}_{\parallel}]$ corresponding to the peak of Fig. 1 for $\Delta=-0.05$ as a function of the position $z_{n\lambda}$ of their centroid. We show results for each of the four bond orientations, $\lambda=1-4$ (diamonds) and for their sum (crosses). The four bonds of the first plane are displaced from their nominal position by 5%. The vertical lines denote the nominal positions of the fcc (100) planes. Notice that the maximum nonlinear polarization is at the second plane $n=2$.

available for different surfaces of Si. For a bulk truncated (100) face we obtained a structureless spectrum which acquired a well defined peak when we allowed for surface relaxation. For the (111) face a much larger peak at a nearby frequency was found even without relaxation. In our calculation, the position of the peak differs from that of the bulk interband transitions due to a local-field-induced shift. Our results also suggest a possible explanation for the lack of sensitivity of the shape SHG spectra on the surface treatment, since they show that the total SH polarization peaks below the first crystalline plane, and it extends for a few other planes before vanishing into the bulk. Appreciable modifications to the polarizability of the first layer change the height of the resonant peak but shift only slightly its position.

In conclusion, our results yield a plausible explanation for the experimentally found SHG resonance. The peak in our model does not arise from a SH transition that becomes dipolarly allowed due to a lattice distortion.[15] Rather, it comes from the large uncompensated local-field gradient at the surface and is therefore allowed even for a centrosymmetrical bond, but within the noncentrosymmetrical environment of the surface. According to our model, the peak observed on the (111) surface is present even without surface relaxation, so its observation should not be interpreted as evidence for a lattice expansion. On the other hand, the peak on the (100) face only arises within our model in the presence of a surface contraction. We remark that with the same parameters our model yields agreement with linear optical anisotropy of Si(110), with the surface and bulk anisotropy of the SHG from Si(111) and Si(100) at 1.17 eV and 2.34 eV, and with the $p \rightarrow P$ SHG spectra of Si(111) and Si(100). In this paper we have restricted our attention to the surface local-field effect, and further theoretical developments would be necessary to find the contributions to SHG from other effects which might also be present.

B.S.M. was partially supported by CONACyT (Grant No. 3246-E9308). W.L.M. was partially supported by DGAPA-UNAM (Grants Nos. IN102493 and IN104594).

[1] J. A. Litwin, J. E. Sipe, and H. M. van Driel, Phys. Rev. B **31**, 5543 (1985).
[2] D. Guidotti, T. A. Driscoll, and H. J. Gerristen, Solid State Commun. **46**, 337 (1983).
[3] T. A. Driscoll and D. Guidotti, Phys. Rev. B **28**, 1171 (1983).
[4] H. W. K. Tom, T. F. Heinz, and Y. R. Shen, Phys. Rev. Lett. **51**, 1983 (1983).
[5] M. A. Varheijen, C. W. van Hasselt, and Th. Rasing, Surf. Sci. **251/252**, 467 (1991).
[6] C. W. van Hasselt, M. A. Verheijen, and Th. Rasing, Phys. Rev. B **42**, 9263 (1990).
[7] C. Jordan, E. J. Canto-Said, and G. Markowsky, Appl. Phys. B **58**, 111 (1994).
[8] R. W. J. Hollering and M. Barmentlo, Opt. Commun. **88**, 141 (1992).
[9] S. V. Govorkov *et al.*, Appl. Phys. A **50**, 439 (1990).
[10] S. V. Govorkov *et al.*, J. Opt. Soc. Am. B **6**, 1117 (1989).
[11] L. L. Kulyuk *et al.*, J. Opt. Soc. Am. B **8**, 1766 (1991).
[12] J. E. Sipe, D. J. Moss, and H. M. van Driel, Phys. Rev. B **35**, 1129 (1987).
[13] G. Lüpke, D. J. Bottomley, and H. M. van Driel, Phys. Rev. B **47**, 10 389 (1993).
[14] G. Lüpke, D. J. Bottomley, and H. M. van Driel, J. Opt. Soc. Am. B **11**, 33 (1994).
[15] W. Daum *et al.*, Phys. Rev. Lett. **71**, 1234 (1993).
[16] J. F. McGilp *et al.*, Opt. Eng. **33**, 3895 (1994).
[17] W. L. Mochán and R. G. Barrera, Phys. Rev. Lett. **55**, 1192 (1985); R. Del Sole, W. L. Mochán, and R. G. Barrera, Phys. Rev. B **43**, 2136 (1991).
[18] W. L. Schaich and B. S. Mendoza, Phys. Rev. B **45**, 14 279 (1992).
[19] E. Palik, *Handbook of Optical Constants of Solids* (Academic Press, New York, 1991), Vol. 1.
[20] Bernardo S. Mendoza and W. L. Mochán (unpublished).
[21] Charlotte E. Moore, *Atomic Energy Levels*, Natl. Bur. Stand. (U.S.) Circ. No. 467 (U.S. GPO, Washington, D.C., 1970), p. 144.
[22] D. E. Aspnes and A. A. Studna, Phys. Rev. Lett. **54**, 1956 (1985).
[23] J. I. Dadap *et al.*, Phys. Rev. B (to be published).
[24] B. S. Mendoza, J. Phys. Condens. Matter **5**, A181 (1993).